

# A 30 MeV H<sup>-</sup> CYCLOTRON FOR ISOTOPE PRODUCTION

R. Baartman, K.L. Erdman<sup>†</sup>, W.J. Kleeven, R.E. Laxdal, B.F. Milton, A.J. Otter, J.B. Pearson,

R.L. Poirier P.W. Schmor, H.R. Schneider and Q. Walker<sup>†</sup>

TRIUMF, 4004 Wesbrook Mall, Vancouver, B.C., Canada V6T 2A9

<sup>†</sup> Ebc Industries Ltd., 7851 Alderbridge Way, Richmond, B.C., Canada V6X 2A4

## Abstract

Because of an expanding market for radioisotopes there is a need for a new generation of cyclotrons designed specifically for this purpose. We describe such a cyclotron currently under construction. It is a 30 MeV H<sup>-</sup> design that exploits a newly developed high brightness multicusp ion source which is capable of H<sup>-</sup> currents of up to 5 mA. This together with careful beam matching then makes feasible accelerated H<sup>-</sup> beam intensities of 500  $\mu$ A. The cyclotron being built is a four sector radial ridge design with two 45° dees in opposite valleys. Beam extraction is by stripping to H<sup>+</sup> in a thin graphite foil. Two extraction probes will allow simultaneous extraction of two beams, each with an intensity of up to 200  $\mu$ A. Energy variation from 15 MeV to 30 MeV is achieved by varying the radial position of the extraction foil.

## 1. Introduction

In an earlier paper<sup>1</sup> we described a preliminary design of a high current H<sup>-</sup> cyclotron for commercial production of radioisotopes. With completion of contractual arrangements between Ebc Industries and Nordion, detailed design and construction of the cyclotron are now under way. The major part of the cyclotron design is being done by TRIUMF, as part of a technology transfer agreement. The cyclotron will be installed in an expansion of the Nordion facility at TRIUMF. The basic specifications for the cyclotron call for a maximum proton energy of 30 MeV, an accelerated beam intensity of at least 350  $\mu$ A, and two external beam lines each capable of currents up to 200  $\mu$ A, and energy variable from 15 MeV to 30 MeV.

## 2. General Description

Figure 1 illustrates the current cyclotron design. It is a four-sector compact design with 38.5° radial ridge hills. The magnet is essentially square in shape with an overall dimension of 2.3 m flat to flat, 1.26 m high and weighs approximately 46 tonnes. It is split at the midplane, allowing four jacks located at the yoke corners to elevate the upper part for access to the cyclotron interior. Two 37,500 At coils mounted on the upper and lower poles provide the magnet excitation. Because of the

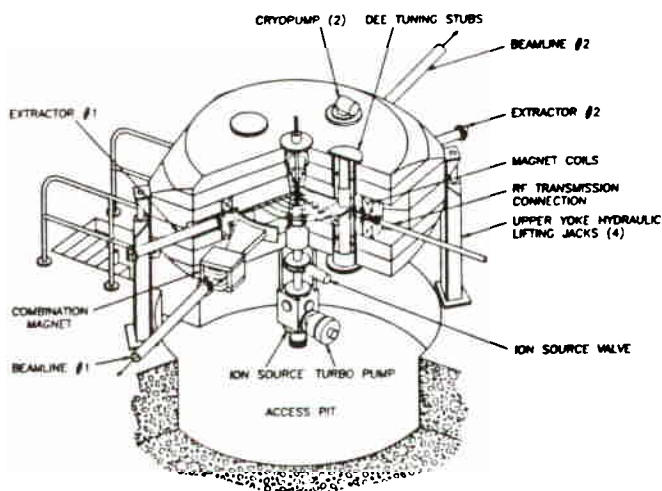


Fig. 1. Cross-sectional and plan views of the cyclotron.

fixed field operation all magnetic field corrections will be made by shimming during construction. No trim coils are planned. Head room requirements in the cyclotron vault are minimized by mounting the magnet over a 1.4 m deep pit and installing the external H<sup>-</sup> ion source and injection line directly below the cyclotron. The H<sup>-</sup> beam is then injected vertically upward along the magnetic axis toward the centre where an electrostatic spiral inflector bends it into the median plane. Two 45° dees located in opposite valleys then provide acceleration at four gap crossings per orbit. The design voltage for the dees is 50 kV, and the operating frequency is 74 MHz, the fourth harmonic of the orbit frequency. The dees operate in phase.

The rf power is delivered to the dees through a capacitive coupling to the 50  $\Omega$  transmission line that passes through a port in the vacuum tank wall. For ease of maintenance the entire rf amplifier system is located outside the cyclotron vault.

Four large holes through the yoke in the dee valleys accommodate the coaxial stubs required to resonate the dees at the operating frequency. For magnetic symmetry there are four identical holes in the unoccupied valleys. Two of these are used as vacuum pump ports in which two 8 in. cryopumps are installed.

The vacuum enclosure is defined by the nickel plated upper and lower pole surfaces and a cylindrical aluminum wall that is sealed to poles with elastomer gaskets. With the pumping provided a pressure of less than  $5 \times 10^{-7}$  torr is expected and beam loss because of gas stripping during acceleration should be less than 3%.

Beam extraction is by stripping to H<sup>+</sup> in thin graphite foils. Two independent external beams are formed with two extraction probes travelling in opposite hill gaps.

Basic parameters for the cyclotron are given in Table I.

## 3. Ion Source

A compact version of the TRIUMF dc volume H<sup>-</sup> multicusp ion source<sup>2</sup> has been tested. After optimizing the magnetic field and the extraction electrodes for this source, it was possible to meet the design criteria for the cyclotron. The extraction electrode aperture was enlarged (compared to that in Ref. 2) to 12 mm diameter in order to reduce the required arc power. The normalized measured beam emittance, for a 5 mA extracted H<sup>-</sup> beam current, is  $0.37\pi$  mm-mrad. This current, measured on a beam stop 2 m downstream of the source, is achieved with  $\approx 2.6$  kW of arc power and 8 std.cc/min of H<sub>2</sub> flow. The current is observed to be stable to  $\pm 2\%$  over periods of 6 h.

## 4. Injection

The energy spread in the external beam will increase with increasing emittance. Therefore, the emittance growth between the source and the extraction foil must be kept small. We do not expect any significant actual emittance growth in the cyclotron but there will be an effective growth due to betatron phase mixing. This is so because the expected phase acceptance from  $-20^\circ$  to  $+20^\circ$  will result in an overlapping of approximately 10 turns at the extraction foil, which means then that the effective emittance at the extraction foil is determined entirely by the maximum beam size at the stripper (provided, of course, that the stripper is sufficiently wide to intercept all of the circulating beam). Any emittance mismatch on the first turn can therefore translate into increased emittance at the extraction foil.

Table I. Principal cyclotron parameters.

Magnet	
Average field	1.2 T
Hill field	1.90 T
Valley field	0.55 T
Hill gap	4 cm
Valley gap	18 cm
Pole radius	76 cm
Number of sectors	4
Ampere-turns	$7.5 \times 10^4$
RF	
Frequency	74 MHz
Dee voltage	50 kV
Harmonic	4
Power	< 35 kW
Vacuum tank	
Pressure	$5 \times 10^{-7}$ Torr
Pumping	4000 $\ell/s$ ( $H_2O$ ), 1500 $\ell/s$ (air)
Ion source	
Type	$H^-$ cusp
Output current	5 mA
Emittance (normalized)	$0.37\pi$ mm-mrad
Bias voltage	25 kV
Extraction	
Energy	15-30 MeV
Method	Stripping
External beams	2

Beam matching at the first turn was studied for a number of inflectors with the electric bend radius  $A$  and the tilt parameter<sup>3</sup>  $k'$  taken as the free design parameters. Using the computer code TRANSOPTR<sup>4,5</sup> the mismatch was minimized by optimizing the  $\sigma$ -matrix (which contains the second moments of the phase space distribution) of the 25 keV beam at the entrance of the inflector, keeping the normalized initial emittance constant and equal to the reference value of  $0.37\pi$  mm-mrad.<sup>6</sup> Transfer matrices for the inflector were obtained using the program CASINO.<sup>7</sup> This is a general inflector orbit code based on a fourth-order Runge Kutta integration routine. In our study the magnetic field was taken as constant (1.2 T) over the entire inflector volume, and a hard edge approximation was used at the inflector entrance. The beam was matched to the acceptance of a dipole with a field index  $n=0.09$ . This is a convenient choice if one wants to study general optical properties. More specific calculations are to be done now that the system design parameters are chosen.

The main results of the calculations are shown in Fig. 2 which gives the growth of the sum of the transverse emittances as a function of the tilt parameter  $k'$ . The two curves for  $A=20$  mm and  $A=25$  mm indicate that the circulating emittances will become larger if one increases the tilt, the electric radius or both (at least for practical values of  $k'$  below  $-1.0$ ). Usually one wants the beam to be centred after it has passed the centre region. This then requires a certain off-centring  $R_c$  at the exit of the inflector. By specifying  $R_c$ , only one of the two parameters  $A$  and  $k'$  can be chosen freely. The two curves given in Fig. 2 for  $R_c=5$  mm and  $R_c=8.5$  mm indicate that in this case the emittance growth is not so much determined by  $k'$  or  $A$  but by the required off-centring, less off-centring giving more emittance growth. We expect that, in our final design, the emittance growth can be kept smaller than a factor 2 to 3. The electrode spacing will be 8 mm. Preliminary envelope calculations indicate that the  $0.37\pi$  mm-mrad entrance beam will pass the inflector with only minor losses.

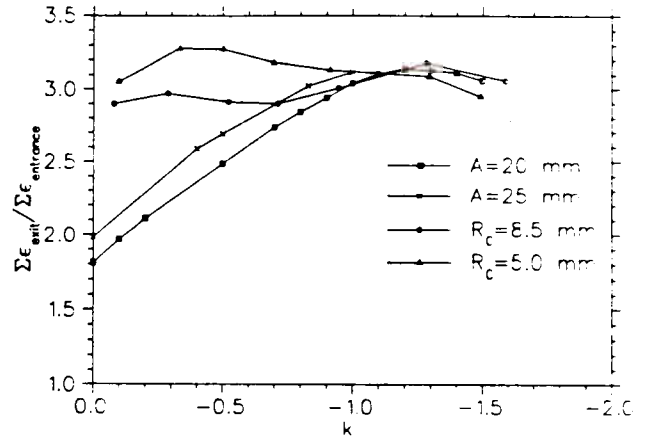


Fig. 2. Growth due to mismatch of the sum of the circulating emittances for an optimized uncorrelated beam at the entrance of the spiral inflector.

In our initial design, the beam line between the ion source and the cyclotron consisted of a solenoid plus a quadrupole doublet. Our TRANSOPTR calculations showed, however, that with this system the optimum  $\sigma$ -matrix at the inflector entrance became harder to generate for highly tilted inflectors, i.e. the best achievable emittances became larger than the predictions following from Fig. 2. Since the emittance growth is due to the transverse coupling in the inflector, it may be anticipated that it can be reduced by starting with a correlated beam at the inflector entrance. One type of correlation can be produced with a skew quadrupole. We did some calculations for a transport line with an additional skew quad between the source and the solenoid. In general we find that the emittance growth can be reduced considerably with this type of correlation. For example, for our reference inflector ( $A=25$  mm,  $k'=-0.83$ ) we found a growth factor of 2.7 for an uncorrelated beam optimized at the inflector entrance. For an optimum setting of the injection line this was 4.0. With the additional skew quad this could be reduced to 1.65. Other advantages of this skew quad are that the beam sizes in the injection line and/or the overall beam line length can be reduced.

## 5. The Central Region

In designing the central region we have tried to maintain good centring for a large phase acceptance, while leaving clearance around the median plane posts for the radial phase space. Transit time effects in the first gap are used to gain phase bunching, thus increasing the size of the accepted phase band by 40%. Special attention was paid to obtaining high energy gain on the first turn to reduce space charge effects, while obtaining small phase-dependent centring errors to avoid coherent emittance broadening. To improve the voltage holding we have maintained a minimum distance between ground and high voltage in the direction perpendicular to the magnetic field of 10 mm except in the injection gap region where it has been cut to 7 mm to reduce the transit time. Finally, we have tried to take advantage of the large  $\nu_x$  at higher energies, by providing a large vertical acceptance at low energies.

Since we wish to avoid using a field bump, the central ray is that which crosses the centreline of the first dee at  $\tau = 0^\circ$  ( $\phi = 0^\circ$ ). This corresponds to a starting time of  $\tau_0 = 41^\circ$ . In Fig. 3 we have shown rays starting at  $\tau_0 = 21^\circ, 31^\circ, 41^\circ, 51^\circ$ , and  $61^\circ$ , superimposed on the equipotential plot of the electric field. The central ray has almost no centring error at turn 10 (2 MeV). The maximum centring error for the other phases in the  $\pm 20^\circ$  phase band is 1 mm and the centring errors are well grouped together in  $x, p_x$  space.

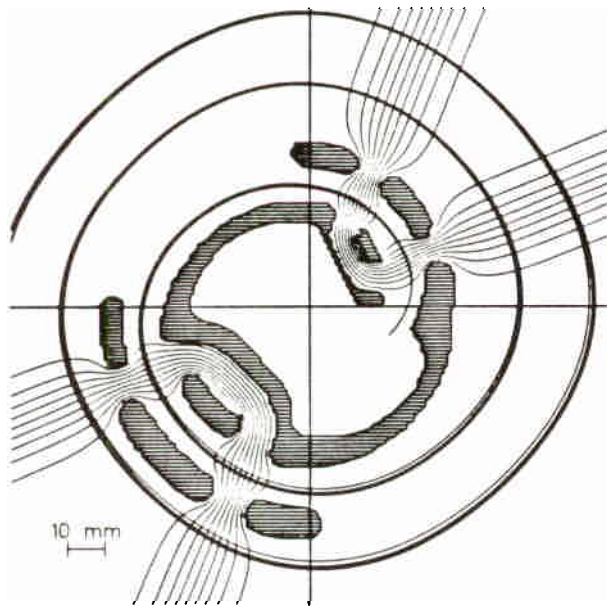


Fig. 3. Orbits of rays with 5 different starting times. Also shown are the central region electrodes in the median plane and the equipotentials of the electric field.

In Fig. 4 the vertical motion is shown for several different phases. In these cases the vertical motion is being treated in the linear approximation, so one need only track two linearly independent rays. We have chosen to show a ray starting with  $p_z=0$  and another with  $z=0$ . The starting values of the conjugate variables have been chosen to show a normalized emittance of  $1.0\pi$  mm-mrad.

#### 6. Beam Extraction

The simplicity of extraction is of course the main attraction of  $H^-$  cyclotrons. It is achieved by passing the  $H^-$  beam through an appropriately positioned thin graphite foil (approximately  $200 \mu\text{g}/\text{cm}^2$ ) to strip off the electrons. The resulting  $H^+$  beam then deflects into the exit channel. For an extraction foil locus that is essentially radial and located in a hill gap as shown in Fig. 1, the  $H^+$  trajectories for the 15 MeV to 30 MeV beams exit the cyclotron through a valley, far from the defocusing effects of the hill fringe fields, and come to a common crossover point outside the magnet yoke. A dipole magnet (combination magnet) placed at the crossover then deflects the extracted beam into the external beam line. Results of transverse phase space computations for a range of extracted beam energies, shows the beams to be well behaved and easily accommodated in a planned 7.5 cm diameter beam pipe.

#### 7. Present Status

Design of the cyclotron is well advanced. Orders have been placed for a number of major components, including the rf amplifier, magnet coils, and magnet steel. Machining of the magnet steel is expected to begin before the end of March 1989. A very tight schedule, calling for two external beams with totally  $250 \mu\text{A}$  by mid 1990, has been set for construction and commissioning of the cyclotron. To assist in any development problems, particularly those related to achieving high beam currents, we are building a central region model, since it is the injection optics and central region where limitations to the accelerated beam currents will occur. Fabrication of the magnet for this

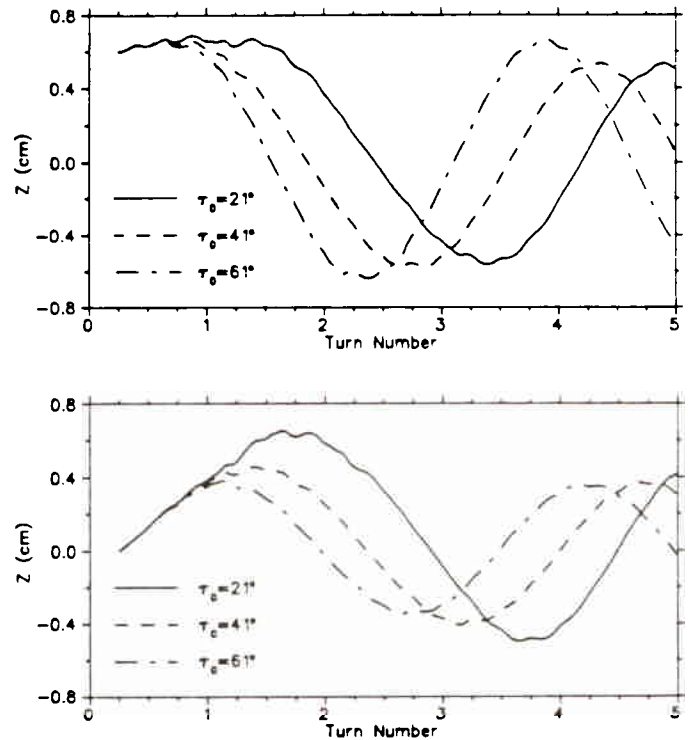


Fig. 4. The vertical motion in the first few turns.

model is nearly complete, and work is proceeding on the dees and injection line components. Existing magnet and rf power supplies will be used.

First beam measurements on the model are expected in July 1989.

#### References

- [1] H.R. Schneider, R. Baartman, R.E. Laxdal, B.F. Milton, A.J. Otter, J.B. Pearson, R.L. Poirier and P.W. Schmor, "A Compact  $H^-$  Cyclotron For Isotope Production", to be published in the proceedings of the first European Particle Accelerator Conference.
- [2] R. Baartman, K.R. Kendall, M. MacDonald, D.R. Moscrop, P.W. Schmor and D. Yuan, "An Intense Ion Source for  $H^-$  Cyclotrons", Proc. 11th Int. Conf. on Cyclotrons and their Applications (Ionics Publishing, Tokyo, 1987), p. 717.
- [3] J.L. Belmont and J.L. Pabot, "Study of Axial Injection for the Grenoble Cyclotron", IEEE Trans. NS-13, 191 (1966).
- [4] E.A. Heighway and R.M. Hutcheon, "TRANSOPTR-A Second Order Beam Transport Design Code with Optimization and Constraints", Nucl. Instrum. Methods 187, 89 (1981).
- [5] M.S. de Jong and E.A. Heighway, "A First Order Space Charge Option for TRANSOPTR", IEEE Trans. NS-30, 2666 (1983).
- [6] R. Baartman, "Matching of Ion Sources to Cyclotron Injectors", to be published in the proceedings of the first European Particle Accelerator Conference.
- [7] B.F. Milton and J.B. Pearson, to be published in the proceedings of the 12th Int. Conf. on Cyclotrons and their Applications, Berlin.

